DISTURBANCE COMPENSATION SYSTEM DESIGN

D. B. DeBra

The design and performance objectives of the Disturbance Compensation System (DISCOS) aboard the TRIAD spacecraft are given. By compensating for the effects of solar radiation and atmospheric drag forces, the DISCOS has increased significantly the accuracy of the predicted ephemerides of TRIAD when compared to those of current operational satellites of the Navy Navigation Satellite System. The DISCOS consists of the following subsystems: controller, proof mass, housing and caging structure, electronics, and propulsion. A detailed description of each subsystem is given, together with the rationale behind the design compromises that had to be made. A brief description of the orbital performance is given which indicates that the design goals have been successfully achieved.

Introduction

THE ACCURACY OF THE NAVY NAVIGATION SATellite (Transit) is dependent on precise orbit determination and its prediction into the future. Further improvements in prediction of the orbit have been limited by the uncertainties in the tiny disturbances from solar radiation pressure and atmospheric drag. These uncertainties are only 10^{-9}g but still are larger than the errors in our current gravity models developed largely from Transit type tracking data. The Disturbance Compensation System (DISCOS) flown on TRIAD has removed this limitation and opened exciting possibilities for improvements in accuracy and operational convenience for the Transit Navigational Satellite system by freeing TRIAD's orbit of disturbances larger than 5×10^{-12}g.

The DISCOS contains an unsupported proof mass that is shielded by the satellite from external forces. Since only gravitational forces act on the proof mass, it follows a purely gravitational orbit. The DISCOS control system senses the motion of the satellite relative to the proof mass and activates thrusters which force the satellite to follow the proof mass without touching it. The satellite therefore follows a purely gravitational orbit free from the effects of external surface forces.

Without the uncertainties which limit current orbit predictions in the operational system to about 12 to 16 hours, the frequency with which the orbit elements must be determined and transmitted to the memory on board the satellite can be reduced to about once a week. Furthermore, the altitude of the satellite can be chosen without regard to drag, at least down to an altitude where the propellant requirements for overcoming drag become too great. Hence, ground coverage, speed of navigational fix, and other altitude considerations need not be compromised by current disturbance limitations. But even with the new demonstrated precision, the orbit will eventually wander from its predicted path. With DISCOS, the satellite follows its proof mass even if it is disturbed. By intentionally disturbing the proof mass through ground commands, it can be made to follow a prepublished ephemeris as long as propellant is available. All of these features have been demonstrated by the DISCOS which is described in this article. The parts of DISCOS are shown schematically in Fig. 1 and as designed in Fig. 2.

DISCOS is another name for "Drag-Free Satellite." Though the idea has been independently proposed several times, B. O. Lange developed the concept while at Stanford University in 1961[1] and studied its application to relativity, geodesy, aeronomy, and other missions.[2] The DISCOS was designed at Stanford University under subcontract to the Applied Physics Laboratory of The Johns Hopkins University to accomplish those improvements. Kent Pugmire and Bob Shaw at AVCO carried out the Stanford design for the propulsion subsystem (with its unusual requirements), and the National Beryllia Corporation did the exacting work of fabricating the very critical pick-off housing.

---

[1] "Conference on Experimental Test of Theories of Relativity," Stanford University, Jul. 20–21, 1961.

[2] B. O. Lange, "The Drag-Free Satellite," *AIAA Journal*, **2**, No. 9, Sept. 1964, 1590–1606.

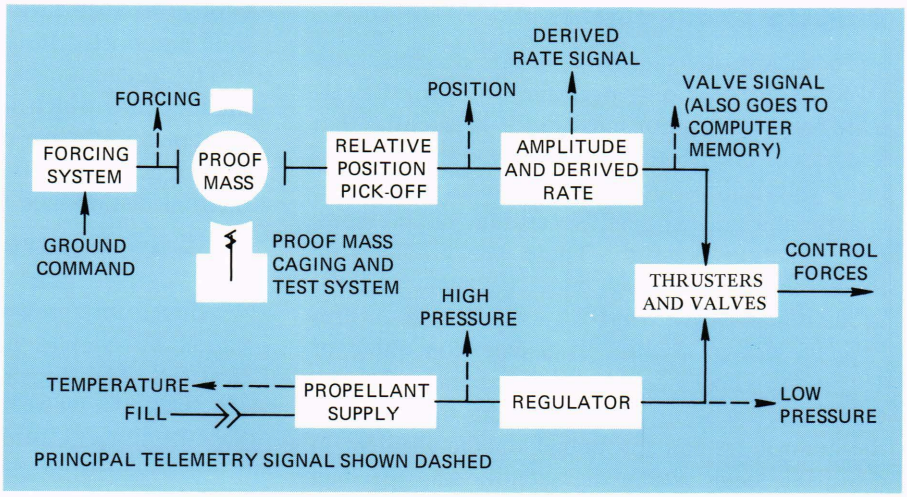

Fig. 1—Block diagram of DISCOS.

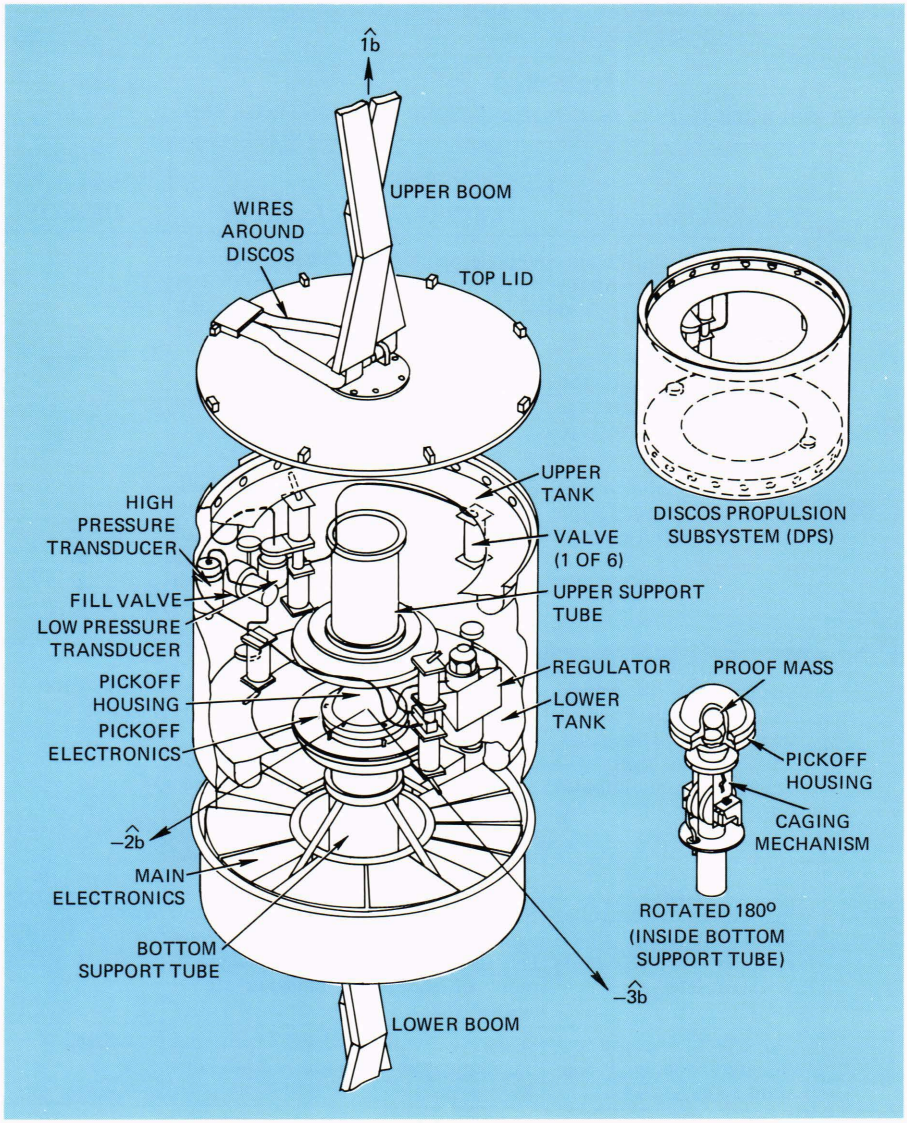

Fig. 2—Exploded view of DISCOS.

DISCOS Requirements

To achieve the successful results obtained with DISCOS, it is not only necessary to make the satellite follow the proof mass but it is essential that it does not disturb the proof mass. Satellite proof mass interactions exist due to mass attraction, electric and magnetic fields, residual gas pressure, and radiation pressure. There are gradients in these forces, too, which must be accounted for in the design of the control system. Based on preliminary design studies, a specification value of 10^{-11}g was chosen for these disturbances. Due to the relative motion inherent in the operation of the control system, the bound on the gradient in disturbing fields within the satellite was specified as 10^{-11}g/mm. The control system was therefore permitted a deadband of 1 mm and is "stiff" enough to keep further displacements to less than 0.25 mm for a disturbance of 10^{-8}g.

The forcing system is limited to 10^{-8}g so that a malfunction, which might leave it on, would not shorten the lifetime of the satellite excessively. It can be adjusted with a resolution as small as the internal disturbance specification value of 10^{-11}g.

DISCOS Controller

A "derived rate" pulse modulation technique, developed for space vehicle attitude control application by Nicklas and Vivian,[3] is used for the thrusters. The thruster on-time is limited by feeding back the valve command (the output of a Schmitt trigger) through a lag circuit. The time

[3] J. C. Nicklas and H. C. Vivian, "Derived-Rate Increment Stabilization: Its Application to the Attitude Control Problem," *J. Basic Engineering, Trans. ASME, Sec. D*, **84**, Mar. 1962, 54–60.

TABLE 1
PARAMETER SELECTION FOR DISCOS DERIVED RATE CONTROLLERS

Parameter	*Symbol*	*Effect on Controller*	*DISCOS Design Tradeoffs*	*Value Chosen For DISCOS*
Turn-on threshold (deadband)	δ_2	Amount of relative motion allowed without thruster activity. Also responsible for about two-thirds of the average displacement of the proof mass when external forces are applied.	Vehicle center of mass movement due to boom flexure of 1 mm or less → δ_2 near 1 mm. Mass attraction gradient of about 0.2×10^{-11}g per mm with a budget of 0.5×10^{-11}g for this effect → δ_2 less than 1 mm.	$\delta_2 = 0.9$ mm
Saturation level	$S = \delta_1 + M\tau_c$	Determines the input value for which the controller is full-on.	Pickoff design considerations indicate a total gap of 9 mm is acceptable. To minimize the possibility of proof mass contact with the wall, very stiff control action near wall must have several mm of full-on before contact.	$S = 6$ mm
Minimum on-time	Δt_{min}	The thruster pulses under most all orbital conditions will be near this duration. Thus, Δt_{min} and thrust level will determine the impulse bit size.	For thrust levels of $\approx 5 \times 10^{-3}N$, want Δt_{min} much longer than valve transient response, but not so long that fuel is wasted in two-sided limit cycles. Also would like the minimum pulse width much larger than the nozzle manifold tailoff time constant of about 9 ms so that thruster tailoff has a negligible effect on stability.	$\Delta t_{min} = 100$ msec
Feedback discharge/charge time constant ratio	$R = \tau_D/\tau_c$	Static gain of controller slightly beyond threshold is $[1/R(S - \delta_2)] \times$ thrust level.	For 5×10^{-3} N force level and external forces of 1×10^{-8}g, want less than 0.25 mm average displacement of the proof mass in steady state.	$R = 25$
Feedback charge time constant	τ_c	No effect if above parameters due held constant (e.g. Δt_{min})	Select a value which facilitates mechanization of both τ_c and $\tau_o = R\tau_c$.	$\tau_c = 2$ sec

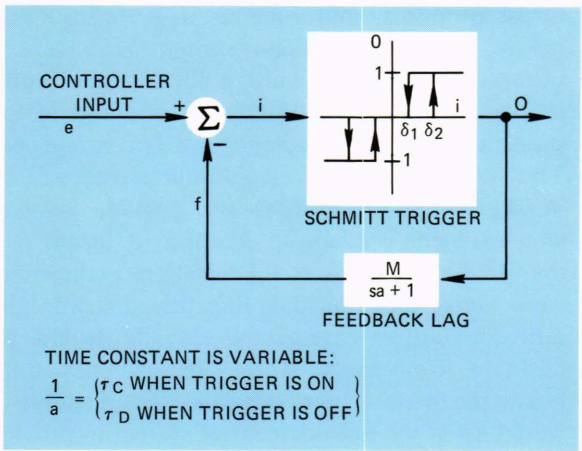

Fig. 3—Simplified schematic of DISCOS derived from rate modulator.

constant of the lag circuit and the trigger hysteresis determine the nominal on-time for typical limit cycle behavior. A block diagram of the controller is shown in Fig. 3. A double-sided Schmitt trigger is activated by a signal i which is the difference between the position sensor output e and a lagged feedback signal f. The thruster is activated by the output o of the trigger. The time constant of the feedback lag is double-valued, the value depending on whether the switch is on (τ_C) or off (τ_D).

The input to the controller e is a function only of proof mass position. Damping of the translational motion is introduced by the feedback signal f, since it is related to the lagged or approximately integrated control acceleration of the thruster. This method of introducing velocity information to the controller reduces the bandwidth requirements on the sensing electronics, thereby making them less sensitive to noise.

The steady state response or static characteristics of the controller to a constant input signal is a train of pulses with both pulse width (p-w) and pulse frequency (p-f) functions of the input magnitude. The principal parameters available to the designer are compared in Table 1. The resulting static characteristics are shown in Fig. 4.

This design has given acceptable performance for the two transient phenomena experienced by the DISCOS. The first is the initial acquisition of the proof mass from the cavity wall to the sensor null which takes approximately 10 minutes. The important performance criterion in this case is a positive acquisition with very little overshoot.

The second kind of transient characteristic is

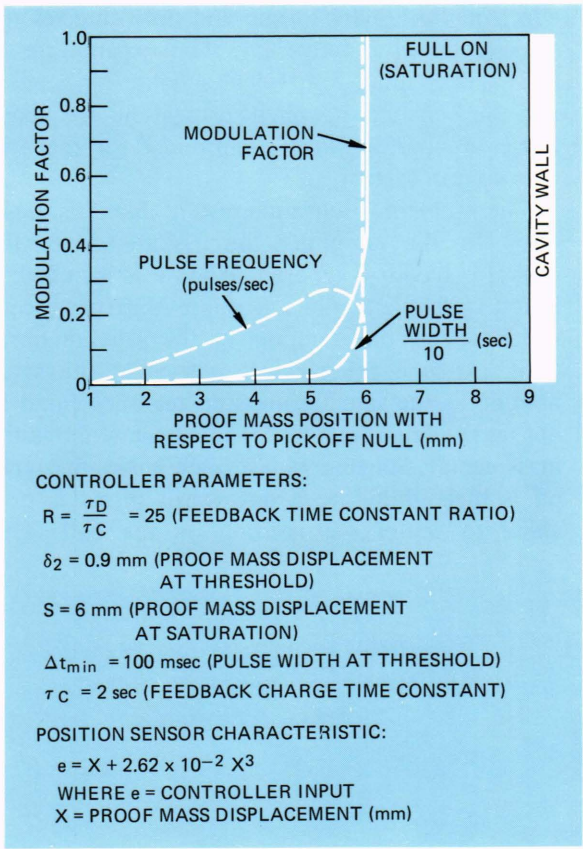

Fig. 4—DISCOS derived rate modulator plus pickoff static characteristics.

the response to a sudden change in the vehicle mass center which results from solar induced thermal bending of the booms. For this kind of disturbance, the low gain of the modulation factor for small error signals prevents excessive propellant consumption, which is important since this occurs twice per orbit. The deadband is intended to provide some insulation against disturbances of this nature, but helps only when the disturbance moves the satellite across the deadband.

Attitude/Translational Coupling

Consider the satellite librations about the pitch axis which is nominally normal to the orbit plane. Neglecting external disturbances, a rotation of the spacecraft results in an error signal which is in phase with the satellite libration. It can cause the thrusters to fire. If the thrust does not pass through the mass center of the satellite, it produces a torque which is either in phase with the libration or 180° out of phase with it. Hence, the torque increases or reduces the magnitude of the

effect of the gravity torque and only changes the satellite libration frequency. The expenditure of fuel is very small for typical satellite parameters and the change in pitch oscillation frequency causes no performance compromise for the attitude control system.

The problem is more interesting than this, however. In the simplified discussion above, the orbital behavior is ignored. When it is included, it is found that a significant phase shift can occur which affects the damping of the satellite librations. Assume the pick-off null is at the same altitude as the satellite mass center but behind it, but let the line-of-action for thrust pass above the mass center. Starting with a pitch angle, the pick-off is high, therefore a downward thrust is provided to center the housing on the ball. This thrust produces no torque as it is vertical and passes through the mass center. However, it pushes the satellite toward a lower, faster orbit so that a little later, the satellite is ahead of the proof mass and a retarding thrust is commanded. This new thrust produces a torque which will be in the same direction as the angular velocity which is being produced by the gravity torque and therefore adds energy to the libration. If the effect were larger than the damping designed into the attitude control system, the satellite would be unstable. Conversely, if the line-of-thrust were below the mass center, this coupling phenomena would assist the attitude control system in providing the necessary damping. Similar, but somewhat more involved arguments provide an explanation of orbital-translation coupling for roll and yaw.

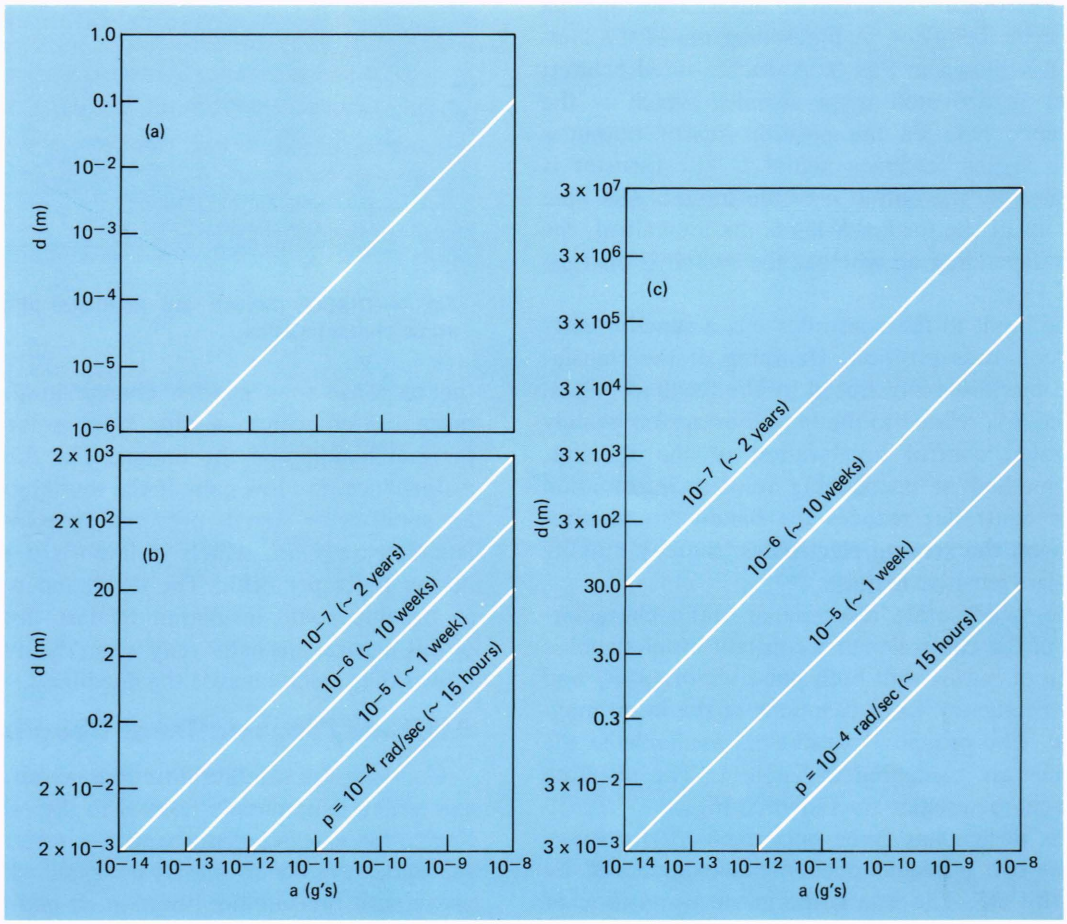

Fig. 5—Orbit perturbation for disturbing acceleration.

(a) Vertical displacement due to a vertical force or normal displacement of orbit plane due to a normal force.

(b) Intrack displacement due to a sinusoidally varying vertical force; F = a cos pt; p < 10^{-3} rad/sec.

(c) Intrack displacement due to a sinusoidally varying intrack force; F = a cos pt; p < 10^{-3} rad/sec.

Unfortunately, there is no combination of parameters that is beneficial to this out-of-plane behavior.[4,5]

Proof Mass Disturbances

Satellite disturbing forces do not have an equal effect in perturbing a satellite from its gravitational path for all directions. The relative effect on perturbations in different directions due to forces acting vertically, intrack, and normal to the orbit plane, are shown for sinusoidal disturbances in Fig. 5. Forces acting normal to the orbit plane displace the orbit plane until the component of gravity, due to the displacement, equals the disturbing force. As long as the disturbances vary slowly compared to orbital frequency (10^{-3} rad/sec) the displacement is independent of time, and is an equilibrium displacement like a force acting against a spring. The same effect occurs for a vertical displacement due to a vertical force. These effects are shown quantitatively in Fig. 5(a). A vertical force changes the radius of the orbit but it also changes its period. This causes the satellite to change its position relative to the gravitational path at a constant rate, and the displacement increases with time. Therefore, a sinusoidally varying vertical force produces a peak error intrack which depends upon the frequency of the disturbance. A similar effect is produced by intrack perturbing forces. In this case, however, the orbital energy is changed; this results in a change in the radius. Both effects result in a single integration, and their quantitative effect as a function of the perturbing frequency is shown in Fig. 5(b). The energy change produced by an intrack force changes the radius linearly; this changes the rate of the displacement intrack linearly. As a result, the intrack displacement increases as a double integration of the intrack perturbing acceleration, and therefore is more sensitive to the frequency of the perturbation. The results are shown quantitatively in Fig. 5(c). One week of constant perturbation at 10^{-11}g produces an amplitude of intrack displacement that is barely detectable by the most advanced satellite tracking systems.

Disturbances intrack due to an intrack perturbation are the most important perturbations to consider. If the body-fixed disturbing forces that act on the proof mass were always aligned with the orbital axes, it would be possible to put a significantly different specification on the disturbance level for each direction. The normal attitude motions, however, allow what is nominally the vertical, or normal axis to have a component along track that would couple as much as 10% of the disturbances in those axes into the intrack direction. For this reason, and because it is very difficult to permit large perturbations in one direction without their appearing in all directions, the specification value for the disturbance level on the proof mass is a single number, and was used as an isotropic design goal.

Perturbations are not always bad. In some cases, a satellite needs to be moved from one station in orbit to another. A constant perturbing force of very small magnitude can produce significant changes as long as it acts in the same direction for a long period of time. In Fig. 6, the effect of constant intrack perturbations is plotted

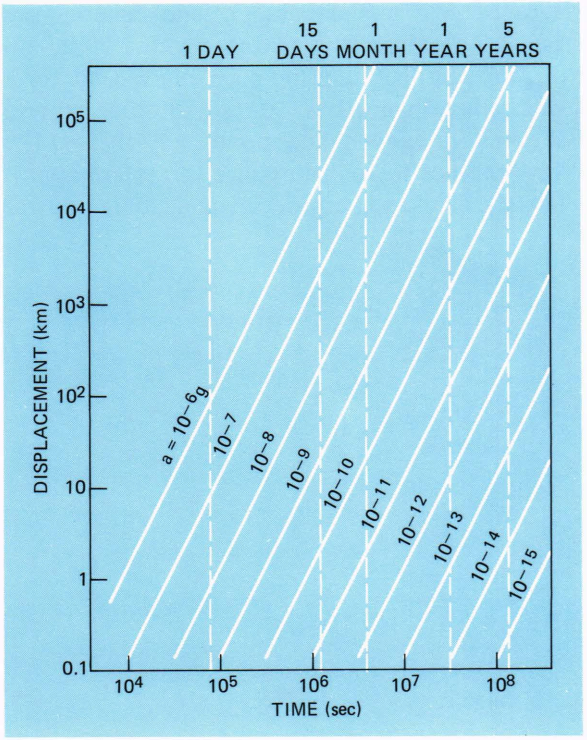

Fig. 6—Intrack perturbations resulting from intrack forces.

[4] A. W. Fleming and D. B. DeBra, "The Stability of Gravity-Stabilized Drag-Free Satellites," *AIAA Guidance, Control, and Flight Mechanics Conference*, Santa Barbara, Calif., Aug. 17–19, 1970.

[5] A. W. Fleming, D. B. DeBra, and M. R. M. Crespo da Silva, "Attitude-Translation Coupling in Drag-Free Satellites," *3rd IFAC Symposium on Automatic Control in Space*, Toulouse, France, Mar. 1970.

as a function of time. These curves may be used to estimate the time required for the proof mass forcing system as discussed later.

Though the proof mass is shielded from the external environment and thus from the large surface force effects of atmospheric and solar radiation drag, there remain many other smaller sources of force on the proof mass. An exhaustive list of these sources, the relationships governing them and calculations of representative magnitudes, have been published by Lange.[2] The dominant force is the mass attraction of the vehicle for the proof mass. This force will be discussed in detail in the following sections. In order of size, the next two effects are the electric field forces of the position sensor and the magnetic force due to magnetic field gradients in the cavity. Other forces produce less than 10^{-13}g disturbance.

By careful design of the position sensor geometry and excitation levels, it is estimated that the electric field specific forces will be no larger than 0.2×10^{-11}g.

The effect of magnetic field gradients can be minimized by minimizing the magnetic susceptance of the proof mass, i.e., by fabricating the proof mass of an alloy of a diamagnetic material such as gold and a paramagnetic material such as platinum. It is estimated that with a 70/30 mix of gold and platinum, the magnetic specific forces will be less than 0.1×10^{-11}g. All other expected specific forces will add up to less than 0.1×10^{-11}g. Since these disturbance forces are approximately of the same order of magnitude and random in direction, the disturbance force budget of the total allowed 1×10^{-11}g is allocated on a root sum square basis. This leaves a budgeted contribution of 0.95×10^{-11}g for mass attraction; for all practical purposes, this can be considered to be 1×10^{-11}g.

If the vehicle could have been built as a perfect sphere of uniformly distributed mass with a hollow cavity at the center, there would be no vehicle mass attraction for the proof mass anywhere in the cavity. This is not practical, but the vehicle mass distribution was made as symmetrical as possible, or parts were kept as far as possible from the proof mass. In this way, there is at least some cancellation of mass attraction forces, and an attenuation due to the $1/R^2$ dependence of the forces. In the DISCOS, for example, all mass—except that associated with the critical functions of the position sensor and caging mechanism—have been placed near the outer skin. Particular attention was given the design and placement of the propellant tanks, since the mass contained in them decreases as propellant is expended. Having two tanks of equal volume and pressure located symmetrically with respect to the proof mass causes these mass attraction forces to cancel; but, in general, the mass attraction force *gradients* of the two masses add, rather than cancel, so the propellant gradient forces at the cavity center would be non-zero and time-varying. The toroidal tanks, however, are a first approximation to a spherical shell when placed just the correct distance apart and they produce no gradient.

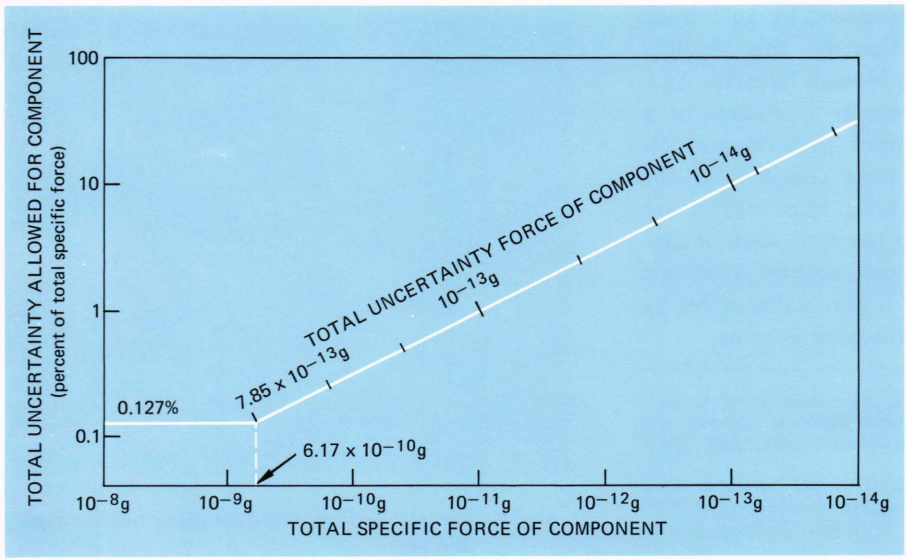

Fig. 7—Component uncertainty allocation.

The error budget for measuring and calculating the effect of each mass was weighted by its size and distance. For sufficiently large masses, no averaging was assumed because there are too few of them. The actual error budget was distributed as shown in Fig. 7.

DISCOS Proof Mass

The proof mass is the heart of the DISCOS System. It does nothing—or at least it tries not to. To minimize the effect of disturbances, it should have the maximum density possible so that for a given surface force, the resulting acceleration is minimized. The ratio of surface to mass decreases linearly with size, and therefore the largest proof mass practical should be chosen. A nominal diameter of 20 mm was chosen and later changed to 22 mm when the gap between the proof mass and pickoff housing was optimized at 9 mm. With a density of 20, a sphere this size has a mass of 111 grams.

Dimensional tolerances on the proof mass are modest and determined primarily by the travel uncertainties permitted in the caging mechanism.

The proof mass must be electrically conductive and must not have a high work function between it and the plate material, so that electrical charges will be drained from the proof mass when it is caged. This is required to minimize electrostatic forces.

To minimize magnetic susceptance of the proof mass, a 70% gold, 30% platinum alloy was used. This, quite happily, was the hardest of the gold-platinum alloys, which made it less likely to be damaged during the caging operation.

DISCOS Proof Mass Housing and Caging

The proof mass housing is the structure that supports the three orthogonal pairs of fixed capacitor plates of the position detection system. Since it encloses the proof mass, it also acts as a structure to which the proof mass is held (caged) during the launch. Its shape is a hollow sphere with an externally projecting equatorial assembly flange. It is fabricated from two hemispheres split on the equatorial plane. One hemisphere has a central indentation for locating the caged proof mass, while the other hemisphere has a diametrically opposed opening through which an indented caging rod (via a spherical bushing) may be inserted for caging and retracted for uncaging the proof mass. The proof mass housing, the caging rod, and the spherical bushing, are made from beryllium oxide (Beryllia B-401). BeO is a stable, strong material. It was chosen because of its light weight, excellent thermal conductivity which minimizes the proof mass disturbances due to a thermal gradient in the residual gases in the cavity, low dielectric constant, and previous experience in working this material for housings and bearings of high precision.

The material blanks were hot pressed in a controlled batch before firing to improve the density uniformity of the material which is expected to approach 0.1%. The internal spherical surface is coated with vacuum deposited chromium, approximately 20,000 Angstroms thick, in the pattern of the required three pairs of orthogonal capacitor plates. The complete external spherical surface and equatorial flange are also chromium coated by vacuum deposition to form an electrical shield.

The caging mechanism performs the dual function of holding the proof mass securely in a known place during launch, and moving the proof mass across the housing cavity in a specific path to allow each of the three orthogonal pickoff axes to be functionally checked prior to launch. This second function requires the vehicle to be within 10° of the vertical launch position since the gravity force is used to keep the proof mass in the caging rod indentation during this motion. In the launch orientation, the intrack axis is horizontal whereas the other two axes are skewed to the vertical. These skewed axes can be exercised by vertical motion but the intrack axis requires special cam action to obtain horizontal movement during caging.

The caging rod is axially moved by a nut and lead screw, and laterally oscillated by a fixed cam so that the proof mass moves in an "S" pattern during the caging or the uncaging cycle. To allow the lateral motion, the lead screw nut and caging rod are interconnected with a pair of intermediate links. These links are made in the form of circular load rings which also serve as the springs which provide a known controlled force on the proof mass in the caged position. This force control is required to prevent overstressing the ceramic proof mass housing and caging rod due to thermal expansion differences acting on the brittle material through the irreversability of the lead screw drive. In the fully retracted (un-

caged) position of the caging rod, the spring links act to hold the caging rod against a hard stop so that its mass position is accurately controlled.

The lead screw is driven by a permanent magnet DC motor, gear reduced so that approximately 30 seconds are required for proof mass motion from the fully uncaged position to the fully caged position (and vice versa). After suitably loading the spring links (at either end position), the lead screw nut actuates a pair of hermetically sealed microswitches which directly break the current driving the motor in that direction. The switch pairs are wired in parallel such that they are redundant when the motor is running but both must operate for breaking the circuit.

The spherical proof mass (11.0 mm radius) is located within six plates forming equal portions of the spherical inside surface of the proof mass housing (20.0 mm radius). The six plates taken in pairs of two form three orthogonal axes with respect to the proof mass housing. The geometry of the six plates can be described as the projection of a cube onto a concentric sphere with 0.8 mm separation for electrical isolation. The gap between the proof mass and housing is 9.0 mm. The proof mass housing's outer wall forms a nearly complete conducting shield around the six electrostatic plates and proof mass. The housing outside diameter is 61.0 mm except at the mounting flange area. The dimensions of the housing are a compromise between the following motivating factors:

1. A large proof mass minimizes the surface force to body forces.
2. A small proof mass minimizes mass and volume.
3. A small gap maximizes the active capacity which minimizes the effect of stray capacity and resulting null drift.
4. A large gap minimizes mass attraction effects and minimizes the probability of the wall touching the proof mass due to a disturbance.
5. A thick wall reduces stray capacity and thermal gradients.
6. A thin wall reduces mass and as a result mass attraction disturbance.

A reasonable range for factors 1 and 2 was chosen as 2-3 cm diameter. The gap was initially large (about 3 cm) and was reduced as dynamic analysis and boom thermal design gave confidence that the gap could be reduced. On this basis, the housing inside diameter was arbitrarily chosen as 4 cm so design could proceed on the longer lead time housing. The ball diameter was finally chosen to maximize the smallest gap (on the side the proof mass is closest to the wall) when there is a null offset. The optimum in this case was for an 11 mm gap which was reduced to 9 mm to reduce the mass attraction gradient force due to a null offset. The result is a 22-mm-diameter proof mass.

The proof mass forms a nearly perfect spherical conductor. The spherical conductor is electrostatically coupled with each of the six plates located on the inside surface of the housing. The size of the spherical conductor relative to the spherical cavity is such that the proof mass radius is comparable to the gap. This condition results in relatively low capacity between the proof mass and each plate.

The diagram below shows an equivalent circuit for one axis of the position detector.

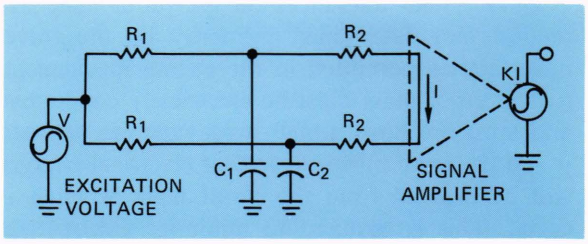

The resistors are packaged with the signal amplifiers. The capacitors shown are made up of three elements: (a) active capacitance, (b) plate-to-shield capacitance, and (c) trim capacitance. Sensitivity increases with both active capacitance and frequency. Active capacitance is limited at 0.31 pF by the control requirement for a large gap between the plate and the proof mass, while frequency is limited to 1 MHz by circuit performance constraints. The position detector was optimized within these two limitations. The approximate sensitvity obtained is 2.9 $\omega\Delta C$ amps/volt for voltages measured from excitation source to proof mass; where ΔC is in farads, and ω is the angular frequency in radians per second.

As the proof mass approaches one of the housing plates, the capacitance from the ball to that plate increases inversely with distance. This condition causes the detector to become nonlinear for large displacements which enhances the desired nonlinearities of the derived rate modulator see Fig. 4).

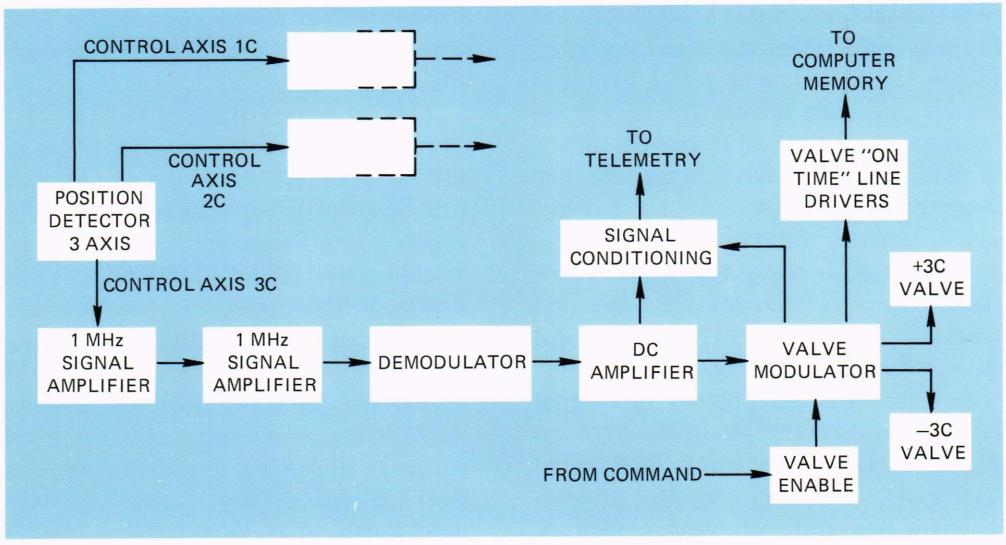

Fig. 8—DISCOS three-axis control system signal flow diagram.

DISCOS Control Electronics

Figure 8 shows a signal flow diagram of the DISCOS control system electronics. There are three nearly identical signal paths in the three control axes. Signals from the three-axis proof mass position detector drive each of three identical differential signal amplifiers. The proof mass position detector, the first two stages of amplification, and the demodulators operate at 1.031 MHz with suppressed carrier amplitude modulated signals. The phase sensitive detectors, or demodulators, convert the 1 MHz proof mass position signals into bipolar differential DC signals. The DC signals are then amplified by means of differential DC amplifiers. The differential DC amplifiers drive the valve modulators which provide proper pulse duty cycle for all control action.

Signal conditioning circuits provide outputs to telemetry of fine and coarse proof mass position signals as well as key parameters from within the valve modulators. The valves may be inhibited or enabled by relay command. Valve "on time" signals are provided for direct transmission to the computer/memory by means of line driver circuits which drive boom cable lines.

Figure 9 shows the DISCOS forcing subsystem. The command system provides 12 bits of data when required by means of a redundant interface. The forcing subsystem redundantly stores 9 of the 12 bits provided. The data are shifted into one of the two registers serially, with the last 9 bits stored and the first 3 shifted out and lost. New data shifted into either register clear any old data that may be present in the redundant register. The data combiner consists of nine "exclusive OR" gates which present 9 bit parallel data from either register to the digital-to-analog converter. Any static failure of any input line, or either storage register, can be handled by the partially redundant subsystem without loss of functional capability. Additionally, a single component failure in the digital-to-analog converter results in only a partial loss of functional capability.

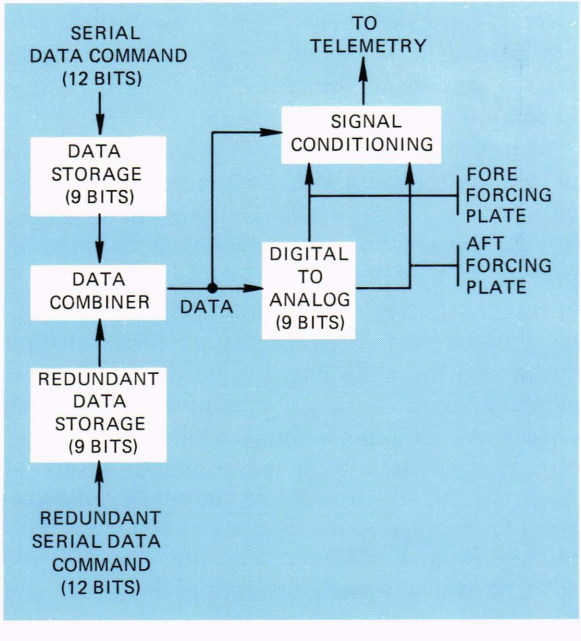

Fig. 9—DISCOS forcing subsystem.

The digital-to-analog converter accepts the 9 bit data (8 bits plus sign) from the data combiner, and provides a linear voltage function for both the fore and aft capacitive plates. The DC voltage on either plate may be varied from zero to 27 volts in steps of 0.106 volt. Voltage may be applied to only one plate at a given time as determined by the polarity bit. Zero forcing corresponds to DC voltage levels of less than 10 mV on each plate. The net force for the maximum forcing command is 1.07×10^{-8} Newton. All force levels are available, both intrack and against track, by command with the polarity bit. Signal conditioning circuits provide telemetry data on both digital and analog forcing levels. The digital data are taken from the data combiner output. The analog data are a direct measurement of forcing voltage at the output of the digital-to-analog converter.

DISCOS Propulsion Subsystem

The DISCOS Propulsion Subsystem (DPS) was designed to operate for one year in an environment having disturbing accelerations of approximately 10^{-8}g caused by aerodynamic and radiation pressure and to settle transients induced by other disturbances such as micrometeorites and thermal boom bending. Sufficient extra propellant was supplied to compensate for a small amount of leakage. The total impulse to meet these requirements is approximately 600 Newton-seconds (Nsec). Thrusters are sized to provide a control force of approximately 5 milli-Newtons. A cold gas propellant was chosen because it distributes itself uniformly in the tanks, which is important in controlling the mass attraction.

It is not practical to operate cold gas systems in a proportional mode at the low flow rates required for the DISCOS. The minimum impulse bit for the system should be made as large as practicable to minimize the total number of valve operations during the mission lifetime. A tradeoff must be made between the amplitude of limit cycles and the allowable deadband size. From a careful analysis of tradeoff studies of performance parameters a nominal impulse bit of 5×10^{-4} Nsec was selected. With the minimum thrust of 5×10^{-3} N, this resulted in the modest requirement for minimum valve on-time of 100 msec. This impulse bit size will require as many as 600,000 solenoid valve actuations during the year, and approximately 100,000 cycles of the low pressure stage of the pressure regulator. An allowable leakage was assigned to each part of the system. The budget was established by arbitrarily allowing 3% leakage.

The propellant used in the DPS is Freon 14 (CF_4). It was chosen because of its high molecular weight (88), and extensive previous use as a propellant in space vehicles. Various mixtures of nitrogen and Freon are standard on a number of satellites; and at an early stage in the DISCOS design, it was decided to preclude any problems of two-phase flow by having the option of using a nitrogen-Freon mixture, if necessary. We did not expect any difficulty with the Freon becoming liquid in the throttling process in the regulator because of the very low flow rates required of DISCOS. In addition, a two-stage regulator was used which could have resulted in some fluctuations from two-stage flow after the first pressure drop, however, none were indicated by the low pressure transducer in flight.

As shown in Fig. 10, the DPS consists of a toroidal tank, a pressure regulator that supplies low pressure propellant to the six thrusters, and associated plumbing and instrumentation.

The only functional interface between the DPS and TRIAD arises from the requirement to fuel the DPS after installation of the payload heat shield just prior to launch. Access to the DPS fill valve is through a 10 in. × 10 in. door in the heat shield, and through an access hole in the APL-DISCOS cylinder, which is the cylindrical support structure that joins the units of the TRIAD during launch.

The DPS has been designed to have less than 10^{-12}g mass attraction on the proof mass. To

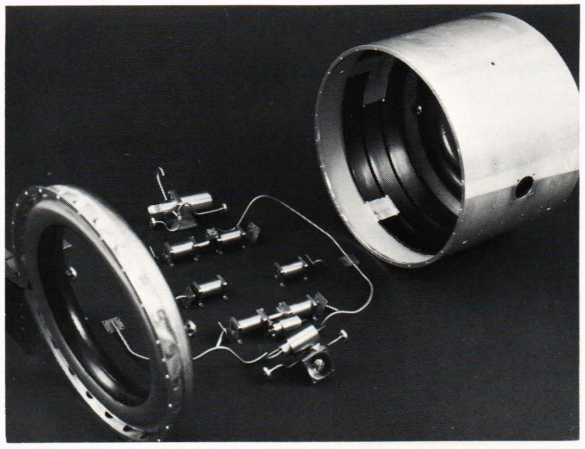

Fig. 10—Unassembled DPS components.

achieve this, a cold gas propellant in toroidal tanks was chosen. The propellant distributes itself uniformly throughout the two toroidal tanks so that the propellant mass center is always at the nominal location of the proof mass, which is at the center and midway between the tanks. Temperature variations over the tanks have been controlled to about 1°C to minimize propellant mass shifts. The double toroidal tank configuration (as opposed to a single one) allows zero gradient in mass attraction at the location of the proof mass. Hence, as propellant is expended, the force of attraction, and its gradient, will remain within the specified design level.

Uncertainties in mass attraction including, for example, variation in wall thickness, density inhomogeneities, the locations of each mass, and for the larger components, their shape, as well as the mass center may be important. For this reason, specified tolerances were unusually small by normal cold gas propulsion system standards.

The distance of the tanks from the proof mass is determined by the requirement for zero gradient at the proof mass and the envelope constraints of the DISCOS structural housing, which must fit inside the APL/DISCOS cylinder. This results in the tanks being mounted on the opposite ends of a cylinder 8.75 inches in length. The tanks are interconnected by high pressure tubing at two locations which also serve as points for a fill connection and for supplying a high-pressure propellant to the pressure regulator. The pressure regulator is accurately located in a bracket which is attached to the structural housing. The positions of the regulator and the fill valve assembly balance the masses of these two fairly large items in crosstrack locations.

Six thrusters are used in the DPS, two in the intrack direction, and four in the vertical and crosstrack directions. The vertical and crosstrack thrusters are located with their axes aligned 45° to the vertical axis in order to provide thrust in the vertical as well as normal to the orbit plane without impinging on the booms. Although the action line of the crosstrack thrusters does not pass through the center of mass of the DISCOS due to the location of the toroidal tanks, the offset is small and results in the expenditure of a negligible amount of extra propellant.

The Assembled DISCOS

The DISCOS structure is essentially two concentric, thin-wall cylindrical tubes, closed on the ends with two thin flat, circular end plates. Since the end plates are axially flexible, stiffness in this direction (between the two cylindrical tubes) is provided by four, symmetrically placed, small-diameter struts that radially connect the concentric tubes at a 45° angle to the cylindrical axis.

This basic structure is supported in TRIAD (for launch configuration) by two circular rings which load the outer cylindrical tube in direct axial compression and the circular, flat, end plates in direct radial tension with uniformly distributed loading.

To take full advantage of this almost ideal structural loading condition, the outer cylindrical tube is used as the primary mounting structure for the large majority of the DISCOS components. About 80% of the total DISCOS mass is concentrated directly on this outer tube and the resulting structural efficiency gives a material volume (weight) whose minimum is limited by thermal conduction requirements rather than mechanical strength.

The two concentric tubes and the two end plates are fully machined parts with tight concentricity control, and are fitted together on precision registry diameters to give a high degree of accuracy in controlling the uniformity of the mass distribution of the basic structure and the mounting location of the individual system components. It is doubtful that a fabricated structure in the conventional sheet and stringer manner could duplicate or even aproach the accuracies that have been thus easily obtained.

The structural material is aluminum alloy 6061-T6. It has the most favorable combination of thermal conductivity, weight, and strength of any material except beryllium, and the ready availability of the sizes and shapes needed, combined with machining ease, also results in minimum cost.

From the standpoint of assembling the modular components into the structure, the DISCOS breaks structurally into three major subassemblies. These are essentially complete, functionally integrated units whose manufacture, assembly, and testing can proceed independently of each other. They are:

1. *The propulsion subsystem.* This is the complete assembly of all mechanical components of the cold gas system onto the inside of the outer

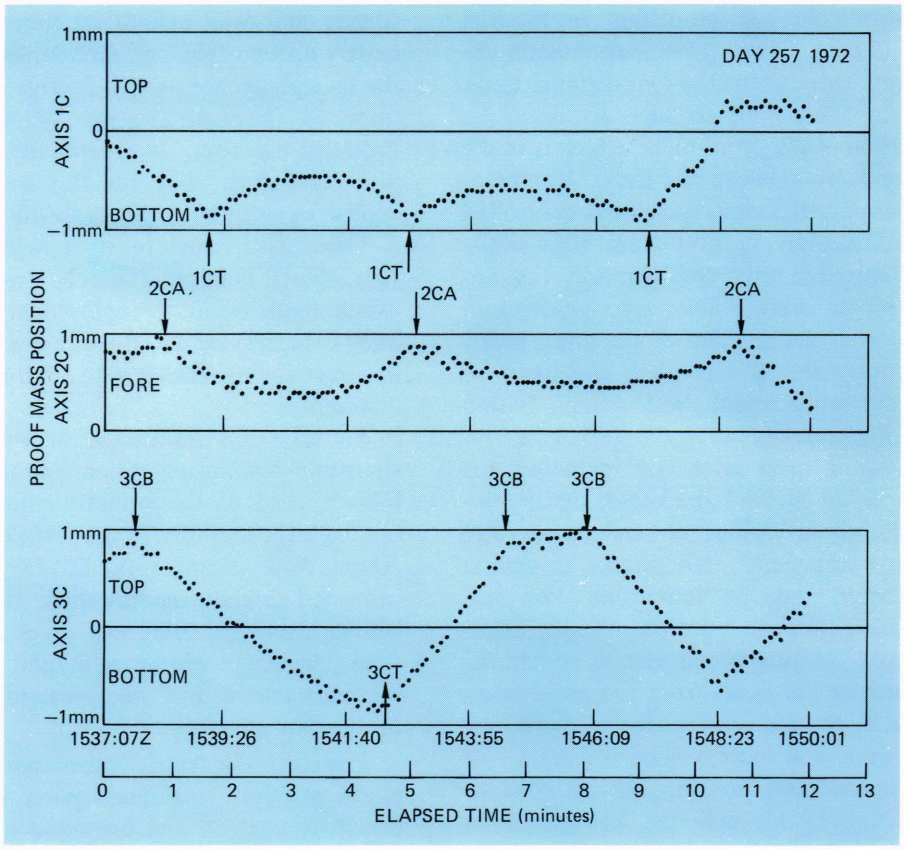

Fig. 11—DISCOS proof mass position, day 257.

structural tube. It may be qualification tested, pressurized, and stored as a separate integrated entity.

2. *The proof mass subsystem.* This is the complete mechanical assembly of the proof mass, proof mass housing, pickoff preamplifier electronics, and caging mechanism into the inner structural tube. It may be mechanically qualification-tested and stored as a separate integrated entity.

3. *The electronic subsystem.* This is the complete mechanical assembly of the electronic modules, electrically connected to each other and assembled onto one of the structural circular end plates. It may be mechanically qualification-tested and stored as a separate integrated entity. It may be electronically qualification-tested with the addition of dummy interfaces with the propulsion subsystem and the pickoff subsystem.

Orbital Performance

The DISCOS operated successfully for one year until it was commanded off. It exceeded its design requirements for orbital perturbations of 10^{-11}g. The resolution of the pickoff was exceedingly good and permitted us to witness the oscillations induced in the booms by firing of these very small rockets. Their 20-second period correlates well with the expected value. Figure 11 shows some typical limit cycles that resulted. The satellite stayed well within its deadband, and was very efficient in its use of propellant. In one case, a large transient behavior in the yaw axis provided us with a way of estimating the location of the mass center that had not been anticipated. This was within specification. Furthermore, the thermal boom bending, which had required us to place a limit of a 1 millimeter deflection on the design of the boom, appeared as expected and within specification.

The DISCOS has not only provided the perturbation-free and adjustable orbit predicted, but has also proved a very interesting and sensitive instrument with which to witness the external disturbances acting on the satellite.